Data Repository DR2009036

Huge Erratic Boulders in Tonga Deposited by a Prehistoric Tsunami

Cliff Frohlich, Matthew J. Hornbach, Frederick W. Taylor, Chuan-Chou Shen, 'Apai Moala, Allan E. Morton, Jens Kruger

This section contains Figure DR1 and Tables DR1, DR2, and DR3.

Section DR1: Dating of coral samples

All coral fossil samples were from erratic boulders sampled on southwestern Tongatapu (Table DR1). Nine carefully selected samples (Table DR2), with ≥ 99 per cent aragonite, were cut, cleaned with ultra-sonic probe for U-Th chemistry (Shen et al., 2003) and isotopic measurements were obtained on a multi-collector inductively-coupled plasma mass spectrometer (MC-ICP-MS), Thermo Electron Neptune. In the High-precision Mass Spectrometry and Environment Change Laboratory (HISPEC), Department of Geosciences, National Taiwan University, we have developed techniques for the MC-ICP-MS that utilize different data acquisition protocols for accurate determination of uranium and thorium isotopic ratios and concentration with 0.1‰-1‰ precision in 1,000-1 picomole quantities. We here employed a triple-spike, ^{229}Th-^{233}U-^{236}U, isotope dilution method to correct mass bias and determine uranium concentration (Shen et al., 2002). The protocol we employed uses one newly-developed MasCom secondary electron multiplier (SEM) with repelling potential quadrupole (RPQ). A sample size of only 1-4 ng U is needed to offer the reproducibility (2 RSD) of 1-2‰ for isotopic measurements. The observation that there is no significant difference between measurements of standards in comparison with the coral and speleothem samples on ICP-sector-field-MS (ICP-SF-MS) and on MC-ICP-MS certify the developed MC-ICP-MS methodology (Fig. DR1). We exclude the dates of two altered samples, FRA1 with a low uranium content of 1.1 ppm and FR2A with a high initial δ^{234}U value of 156.2 ± 2.4 (Table DR2).

Section DR2: Estimating wave height

Several investigators have developed relationships of varying complexity to estimate the minimum necessary heights for storm and tsunami waves in terms of the boulder's three linear dimensions and three hydrodynamic coefficients that describe the flow (e. g., Nott and Bryant, 2003; Noormets et al., 2004). In the text for Boulder #1 we apply Nott and Bryant's (2003) Equations (13) and (14), and obtain minimum wave height h_w estimates of 44 m and 19 m assuming boulder dimensions *a*, *b*, and *h* of 15 m, 11 m, and 9 m, drag, lift, and inertial coefficients C_d, C_l, and C_m of 1.2, 0.178, and 1.0, boulder and water densities ρ_b and ρ_w of 2.0 and 1.02 g/cm^3, and $\ddot{u}$ of 1.0 m/s^2.

A similar but much simpler calculation obtains approximately the same result. If we assume that water in a wave has potential energy *mgh* when it impacts a shoreline where it loses altitude *h* and is converted to kinetic energy $mV^2/2$, and that the flow must have velocity *V* up to some fraction *F* of the boulder's height then:

$$\frac{1}{2}mV^2 = mg(h_w - Fh_b)\,. \qquad \text{(DR1)}$$

The flow velocity *V* must be such that the drag force exceeds the boulder's weight. For a boulder of height and width h_b, the cross section *A* is $\sim h_b^2$; if the boulder's density is ρ_b, the water density is ρ_w, and the drag coefficient is *C*, this assumption is:

$$\frac{1}{2}C\rho_w h_b^2 V^2 > g(\rho_b - \rho_w)h_b^3\,. \qquad \text{(DR2)}$$

Eliminating *V* from these two equations indicates the minimum wave height h_w to move a boulder will be:

$$h_w > \left[\frac{1}{C}\left(\frac{p_b}{p_w} - 1\right) + F\right]h_b\,. \qquad \text{(DR3)}$$

If one arbitrarily assumes that *C* and *F* are both about 1.0, then:

$$h_w > \frac{\rho_b}{\rho_w}h_b\,; \qquad \text{(DR4)}$$

i. e., the size of a wave to move a boulder of given density and height is proportional to the product of the boulder's relative density and its linear dimension.

For Boulder #1 this gives a minimum wave height of 20-25 m. Given the practical uncertainties concerning densities, drag and lift coefficients, etc., this result may be about as accurate as Nott and Bryant's (2003). Both make questionable assumptions about details but depend fundamentally on the principal that motive forces depend on flow velocity and after a wave reaches shore flow velocities depend on wave potential energy.

Section DR3: Computer modeling

For our tsunami modeling, for the gridded bathymetry we use General Bathymetric Chart of the Oceans (GEBCO) data with one arc-minute resolution for deep (> 500 m water depths) and SOPAC multibeam data with 30 m resolution in shallow water.

For volcanic flank collapses and slumps, all modeled slides are rotational, occur along near-vertical faults, and produce maximum slide accelerations according to Watt's slide model (Watts et al., 2005). We assume a terminal sliding velocity of 40 m/s. We use headwall lengths measured directly from bathymetric data to estimate slide thickness and slide diameter. Given the moderately poor constraints on slide size, slide volumes may be either larger or smaller than tabled values (Table DR3) and run-distances may also vary. Any increase in slide volume will cause a scaled increase in wave amplitude.

For earthquakes, we modeled tsunamis generated by hypothetical moment magnitude M_W 9 earthquakes along both the Tonga and New Hebrides trenches. Our strategy was to specify fault geometries and locations consistent with regional seismicity and geology, and place the faults at the minimum depth so as to produce the maximum uplift of the ocean floor. Thus the hypothetical earthquakes had centroid depths of 35 km and slips of ~30 m along faults dipping at 30° with dimensions ~120 km **x** 1000 km. For sources along the Tonga trench the resulting tsunami impacts the eastern shores of Tongatapu and other islands in the Tonga arc with waves of up to 24 m (peak-to-trough) at the 100 m contour. The wave is considerably smaller (<12 m) at Fahefa and elsewhere on the west side of the islands. Similar models of M_W 9 earthquakes along the New Hebrides trench generated even smaller (<1 m) waves impacting Tonga, mainly because regional bathymetry defocuses the waves away from western Tongatapu.

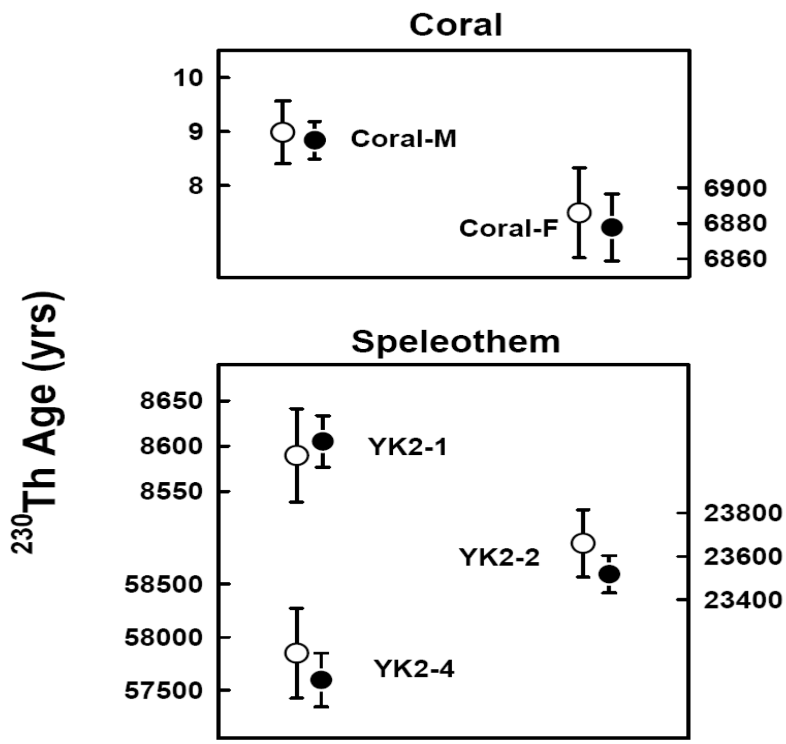

Figure DR1. Validation of age-determination method. Comparison of ^{230}Th ages determined on ICP-SF-MS (hollow circles, Shen et al., 2002) and MC-ICP-MS (solid circles) for two coral *Porites* samples, Coral-M and Coral-F, collected from Nanwan, southern Taiwan, and three subsamples, YK2-1, YK2-2, and YK2-4, of one stalagmite, YK2, collected from southwestern China. All data are consistent within error.

Table DR1. Locations and basic characteristics of erratic boulders on southwestern Tongatapu. Latitudes and longitudes are determined using a handheld GPS instrument. Except as otherwise indicated, elevations and distances to shoreline are determined from Tonga Ministry of Land, Survey, Natural Resources and Environment, map series 2007. Heights are estimated by inspection or measured with a tape; circumferences are as measured with a tape. *Samples selected for x-ray analysis.

boulder #	*lat (°S)*	*long (°W)*	*nearby village*	*elevation (m above mean high tide level)*	*distance to shoreline (m)*	*orientation*	*height (m)*	*circum-ference (m)*	*base undercut*	*samples collected*
1	21.13496	175.34485	Fahefa	9.4[a]	130	upright	9 m	> 45 m (measured below greatest diameter)	yes	FRA1* FRB1 FRC* FRD FRE FRF* FR1F*
2	21.13376	175.34422	Fahefa	14[a]	240	upright, but tilted	4	23 m		FR2A* FR2B FR2C
3	21.14313	175.34070	Fahefa	19±3	280	upright	4	42	yes	FR3A FR3B*
4	21.14636	174.33991	Fahefa	~20	430	upright	3-4	14	yes, one side	FR4A*
5	21.14605	175.33991	Fahefa	~20	380	upright	5	23	yes, one side	FR5A*
6	21.14560	175.33913	Fahefa	~20	390	overturned	2-3	19	yes	FR6A
7	21.15320	175.33767	Fahefa	14±3	160	overturned	5	35	yes	FR7A*

[a]Elevations determined by geodetic leveling.

Table DR2. Uranium and thorium isotopic compositions and ^{230}Th ages for Tonga coral fossils. These data are from measurements on the MC-ICPMS at the Department of Geosciences, National Taiwan University. Analytical errors are 2σ of the mean.

Sample ID	Weight g	^{238}U ppb		^{232}Th ppt		δ^{234}U measured[a]		[^{230}Th/^{238}U] activity[b]		[^{230}Th/^{232}Th] ppm[c]		Age uncorrected		Age corrected[b,d]		δ^{234}U$_{initial}$ corrected[e]	
FRA1	0.0525	1113.3[f]	± 1.9	597	± 13	104.8	± 1.4	0.7974	± 0.0024	24553	± 553	135,241	± 882	135,228[f]	± 882	153.6	± 2.1
FRC	0.0540	2830.6	± 3.9	2380	± 14	104.1	± 1.6	0.7824	± 0.0019	15364	± 95	130,612	± 737	130,592	± 737	150.6	± 2.4
FR1F	0.0965	1909.0	± 1.9	1681	± 8	98.9	± 1.3	0.7520	± 0.0015	14097	± 69	122,647	± 531	122,627	± 531	139.8	± 1.9
FRF	0.0641	2233.2	± 3.4	1184	± 11	100.7	± 1.6	0.7660	± 0.0017	23849	± 226	126,433	± 642	126,421	± 643	143.9	± 2.3
FR2A	0.0460	2700.0	± 4.8	1009	± 15	105.9	± 1.6	0.8052	± 0.0021	35586	± 544	137,493	± 827	137,485[g]	± 827	156.2	± 2.4
FR3B	0.0634	2156.2	± 2.9	1383	± 11	106.8	± 1.4	0.7809	± 0.0017	20107	± 167	129,482	± 624	129,467	± 624	154.0	± 2.0
FR4A	0.0544	2127.6	± 3.4	2033	± 13	104.8	± 1.5	0.7655	± 0.0020	13226	± 92	125,289	± 689	125,267	± 690	149.3	± 2.2
FR5A	0.0792	2205.7	± 2.8	1496	± 9	105.0	± 1.5	0.7696	± 0.0016	18730	± 119	126,455	± 587	126,439	± 587	150.1	± 2.1
FR7A	0.0498	2063.8	± 3.4	1392	± 14	105.2	± 1.5	0.7691	± 0.0019	18830	± 196	126,264	± 685	126,249	± 686	150.3	± 2.2

[a] $\delta^{234}U = [^{234}U/^{238}U]_{activity}$

[b] $[^{230}Th/^{238}U]_{activity} = 1 - e^{-\lambda_{230}T} + (\delta^{234}U_{measured}/1000)[\lambda_{230}/(\lambda_{230} - \lambda_{234})](1 - e^{-(\lambda_{230} - \lambda_{234})T})$, where T is the age.

[c] The degree of detrital ^{230}Th contamination is indicated by the [^{230}Th/^{232}Th] atomic ratio instead of the activity ratio.

[d] Decay constants are 9.1577×10^{-6} yr^{-1} for ^{230}Th, 2.8263×10^{-6} yr^{-1} for ^{234}U, and 1.55125×10^{-10} yr^{-1} for ^{238}U (Cheng et al., 2000). Age corrections were calculated using an ^{230}Th/^{232}Th atomic ratio of 4 (± 4) ppm. Those are the values for a material at secular equilibrium, with the crustal ^{232}Th/^{238}U value of 3.8. The errors are arbitrarily assumed to be 100%.

[e] $\delta^{234}U_{initial}$ corrected was calculated based on ^{230}Th age (T), i.e., $\delta^{234}U_{initial} = \delta^{234}U_{measured} \, X \, e^{\lambda_{234} * T}$, and T is corrected age.

[f] [^{238}U]: anomalously low

[g] $\delta^{234}U_{initial}$: anomalously high

Table DR3. Parameters used for modeling slides and volcanic flank collapse.

Model Parameter	*Slide 1*	*Slide 2*	*Volcano 1*
type	rotational slump	rotational slump	rotational slump
diameter of Gaussian (2σ) (m)	500	1030	4000
maximum thickness (m)	50	100	200
approx. initial depth of failure (m)	140	450	400
approx. final stopping depth (m)	200	600	500
slide duration (s)	6	4	10
maximum speed (m/s)	40	32	40
distance from Fahefa shoreline (km)	0.18	5	35
wave travel-time to shoreline (sec)	10	80	310
peak-to-trough amplitude at 100 m contour (m)	10	4.8	14
Peak-to-trough duration At 100 m contour (sec)	21	40	80

Additional References

Cheng, H., Edwards, R.L., Hoff, J., Gallup, C.D., Richards, D.A., Amerom, Y., 2000, The half-lives of uranium-234 and thorium-230: Chemical Geol., v. 169, p. 17-33.

Noormets, R. Crook, K.A.W., and Felton, E.A., 2004, Sedimentology of rocky shorelines: 3. Hydrodynamics of megaclast emplacement and transport on a shore platform: Oahu, Hawaii: Sedimentary Geol., v. 172, p. 41-65, doi:10.1016/j.sedgeo.2004.07.006.

Okada, Y., 1985, Surface deformation due to shear and tensile faults in a half-space: Bulletin of the Seismological Society of America, v. 76, p. 1135-1154.

Shen, C.-C. et al., 2002, Uranium and thorium isotopic and concentration measurements by magnetic sector inductively coupled plasma mass spectrometry: Chemical Geol., v. 185, p. 165-178, doi:10.1016/S0009-2541(01)00404-1.

Shen, C.-C. et al. , 2003, Measurement of attogram quantities of ^{231}Pa in dissolved and particulate fractions of seawater by isotope dilution thermal ionization mass spectroscopy: Anal. Chem., v. 75, p. 1075-1079, doi:10.1021/ac026247R.

Watts, P., Grilli, S.T., Tappin, D.R., and Fryer, G. J., 2005, Tsunami generation by submarine mass failure part II: Predictive equations and case studies: Journal of Waterway, Port, Coastal, and Ocean Engineering, v. 131, p. 298-310, doi: 10.1061/(ASCE)0733-950X(2005)131:6(298).